SSRG International Journal of Electronics and Communication Engineering
ISSN: 2348-8549/ https://doi.org/10.14445/23488549/IJECE-V13I6P106

Volume 13 Issue 6, 65-77, June 2026

Original Article

Physics-Constrained Inverse Antenna Design with Hardware-Deployable Intelligence for Real-Time IoT Systems

C. Rajan[1], M. Kavitha[2*], Shaik Sadulla[3]

[1]*Department of CSE (AIML), K.S Rangasamy College of Technology, Tiruchengode, India.*
[2]*Department of Electronics and Communication Engineering, Saveetha School of Engineering, Saveetha University, Chennai, India.*
[3]*Department of Electronics and Communication Engineering, KKR & KSR Institute of Technology and Sciences, Vinjanampadu, Guntur, Andhra Pradesh, India.*

**Corresponding Author : mkseee2007@outlook.com*

Received: 08 March 2026 Revised: 07 April 2026 Accepted: 06 May 2026 Published: 27 June 2026

Abstract *- Internet-of-Things (IoT) platforms require compact and adaptive antennas to work within a tight size, power, and cost-sensitive set of constraints. The traditional design of an antenna is based on the forward Electromagnetic (EM) optimization, which is computationally expensive and cannot be used in real-time adjustment. Intelligent methods based only on data, though efficient, do not always take into consideration physical aspects and the deployability of hardware. The paper suggests a physics-constrained system of inverse antenna design where intelligent inference is applied as a solution- enabling methodology, instead of the new paradigm. The antenna desired specifications are invertedly synthesized to physically valid antenna design parameters by an inverse synthesis method, which explicitly applies EM, fabrication, and deployment constraints. The proposed architecture combines a lightweight, physically deployable inference engine and a constraint certification loop based on physics, which is safe and reliable to generate the antenna. The inverse synthesis accuracy is verified using electromagnetic simulation on a set of patch antennas on a microstrip basis, where the mean relative error of resonant frequency and resonant |human| at resonance were 0.25 GHz and 2.5 dB, respectively. The certification loop of physics also discards non-feasible geometries, but the rate of constraint violation is lessened to 21 per cent (unconstrained inverse) and 0 per cent (proposed). Hardware deployability is also exhibited by the 8-bit fixed-point quantization of the inference engine and 12,000 parameters, which needs 48 kB of memory and 0.15 ms inference latency, and supports real-time on-device synthesis on an IoT platform.*

Keywords *- Inverse Antenna Design, Physics-Constrained Intelligence, Hardware-Deployable Inference, Iot Antennas, Real-Time Antenna Tuning, Vlsi-Aware Intelligent Systems.*

1. Introduction

Compact and adaptive antennas are needed to ensure the stability of Internet-of-Things (IoT) communication systems with stringent size, power, latency, and deployment requirements [1-4]. New IoT systems are in need of antennas that can dynamically change their electromagnetic response to a changing environment, spectrum congestion, as well as the compact size of devices that need to be integrated [5-7]. Nevertheless, the design of antennas is not easy since the electromagnetic performance is significantly influenced by the coupled geometrical, material, fabrication, and deployment variables.

Conventional antenna design procedures largely depend on forward Electromagnetic (EM) optimization with the help of full-wave simulation, parametric sweeps, and tuning [8-10]. These approaches are computationally expensive and cannot be used in real-time or embedded IoT adaptation, though they give accurate results. Recent developments in machine learning and intelligent antenna synthesis have presented surrogate-assisted optimization and inverse learning techniques to speed up antenna design [11-16]. Still, most of the current solutions are not constrained and can produce geometries that are out of bounds on fabrication and passivity, compactness, or deployment ability [17-19].

Inverse electromagnetic design is a relatively new, appealing alternative, which transfers the specifications of target antennas onto the geometries of physical antennas [20-24]. Nevertheless, the currently available inverse design methods also have various drawbacks, such as unconstrained learning formulations, expensive computations, and a lack of

support towards embedded implementation in real-time [25-27]. Simultaneously, advances in edge computing and ultra-low-power VLSI systems have made lightweight intelligent inference possible on embedded IoT systems [15, 28-32]. The majority of existing research, despite these innovations, is either more electromagnetically accurate or hardware-efficient inference, but lacks physics-constrained synthesis and real-time deployability in one model [33-35]. Thus, there remains a considerable research gap in the development of an inverse antenna synthesis model that not only ensures physical feasibility and fabrication safety but also hardware-deployable real-time performance of IoT systems [36-43].

This paper seeks to fill this gap by offering a physics-constrained framework of inverse antenna design with hardware-deployable intelligence to real-time IoT systems. The framework proposed directly maps antenna geometry, based on target specifications, with a lightweight inverse intelligent inference engine and implements electromagnetic, fabrication, and deployment constraints via a deterministic, projection-based certification mechanism. The proposed method, as opposed to unconstrained inverse learning methods, ensures physically achievable antenna geometries prior to implementation. Also, 8-bit fixed-point quantization is used to implement the inference engine in order to enable low-memory and low-latency embedded operation. This work has novelty in that it combines inverse antenna synthesis with deterministic physics-constrained certification with hardware-aware intelligent deployment in a single framework. The proposed method, in contrast to traditional forward optimization methods, allows direct synthesis with rapid repetition of EM optimization.

In contrast to unconstrained inverse learning algorithms, it can remove infeasible generation of antennas with explicit projection-based feasibility enforcement. In addition to that, in contrast to current intelligent antenna synthesis efforts where electromagnetic accuracy is a primary consideration, this paper directly assesses hardware deployability based on memory footprint, inference latency, and quantization analysis.

The most important contributions of this work are as follows:

1. To map target antenna specifications to physically feasible antenna geometries, a physics-constrained inverse antenna synthesis framework is constructed that directly maps target antenna specifications to an antenna geometry.
2. To implement electromagnetic, fabrication, and deployment feasibility constraints, a deterministic projection-based certification mechanism is proposed.
3. An inverse inference engine is developed as a hardware-deployable, lightweight 8-bit fixed-point quantization-based inference engine to implement in real time in the IoT.
4. Detailed simulation-based analysis is performed with electromagnetic validation, constraint-compliance analysis, hardware feasibility analysis, and comparison with forward optimization and unconstrained inverse learning algorithms.

The remaining paper is structured in the following way. Section 2 discusses related literature on antenna optimization, inverse electromagnetic design, and hardware-intelligible intelligent systems. Section 3 shows the proposed framework and approach. Section 4 talks about electromagnetic validation, comparative analysis, and hardware feasibility. Lastly, Section 5 is a conclusion section of the paper and a plan of future research directions.

2. Literature Review

Previously existing studies on antenna design have mainly been concerned with forward EM optimization and measurement-based refinement, which, despite being accurate, lack scalability and convergence speed in complex/adaptive systems [8-10]. Development of computational intelligence in antenna engineering has resulted in surrogate-assisted modelling, sensitivity-directed optimization, as well as learning-based parameter exploration, which have significantly decreased design time [11-16]. However, most of these methods are more focused on predicting performance and not synthesizing performance, and they tend to ignore the issue of constraint enforcement, leading to a design that does not validate either physically or fabricated [17-19].

Inverse EM design has recently been studied in RF, photonic, and plasmonic systems and has shown that deep learning and surrogate models can be used to directly produce target responses with a structure [20-27]. Most inverse design frameworks are still computationally expensive or do not connect with real-time embedded execution, despite these advances, and cannot be adopted in IoT systems [25-27]. Meanwhile, intelligent and reconfigurable antenna systems research has explored the topics of metasurfaces and movable radiators as well as adaptive beamforming to improve spectral efficiency and sensing performance [5-7, 33-35]. These systems are, however, usually based on external controllers or offline optimization and are not closely integrated with hardware- aware intelligence. On the hardware side, there has been widespread research on energy-efficient and PPA-optimised VLSI architectures to enable real-time intelligent processing at the edge [15, 28-32]. The idea of learning-guided design automation, TinyML co-design, and hardware-efficient signal processing pipelines has proven that it is possible to implement intelligent models within a limited set of resource constraints [15, 29-32, 36-38]. Although these attempts solve the deployability, they are not often combined with the EM-sensitive or physics-limited antenna synthesis. Consequently, there is still an unclear research gap in creating

the framework of antenna designs that can simultaneously tackle inverse EM synthesis, certifying physical constraints, and intelligence in hardware that can be deployed in real- time to IoT platforms [39-43]. In contrast to the currently present physics-informed or inverse-learning antenna techniques, this study implements hard feasibility through deterministic Projection and not soft penalty. Current research has enhanced optimization of antennas with machine learning, inverse electromagnetic synthesis, and hardware-conscious intelligent systems, but there are still a number of weaknesses. Forward EM optimization techniques are very accurate but need computationally intense full-wave simulations [8-10]. AI-aided and inverse learning techniques decrease design time, but do not usually ensure physical feasibility and fabrication safety [11-27]. Likewise, hardware-conscious intelligent systems are primarily concerned with low-power embedded inference with no consideration of physics-constrained antenna synthesis [15, 28-32]. This means that there is a gap in research towards a framework that integrates inverse electromagnetic synthesis, deterministic physics-based enforcement of constraints, generation of antennas that are fabrication-safe, and a hardware-realizable real-time inference into IoT systems. The given gap is filled in the proposed work by the projection-based physics certification, which is combined with lightweight inverse intelligent inference.

3. Methodology and Experimental Setup

3.1. System-Level Framework Overview

The proposed methodology is based on an end-to-end inverse antenna synthesis framework, which closely incorporates electromagnetic modeling, physics-motivated constraint- imposing, and hardware-deployable intelligent inference. Desired antenna performance parameters, including operating frequency band, matching level of impedance, and radiation efficiency, are keyed in and directly synthesized to physically feasible antenna design parameters.

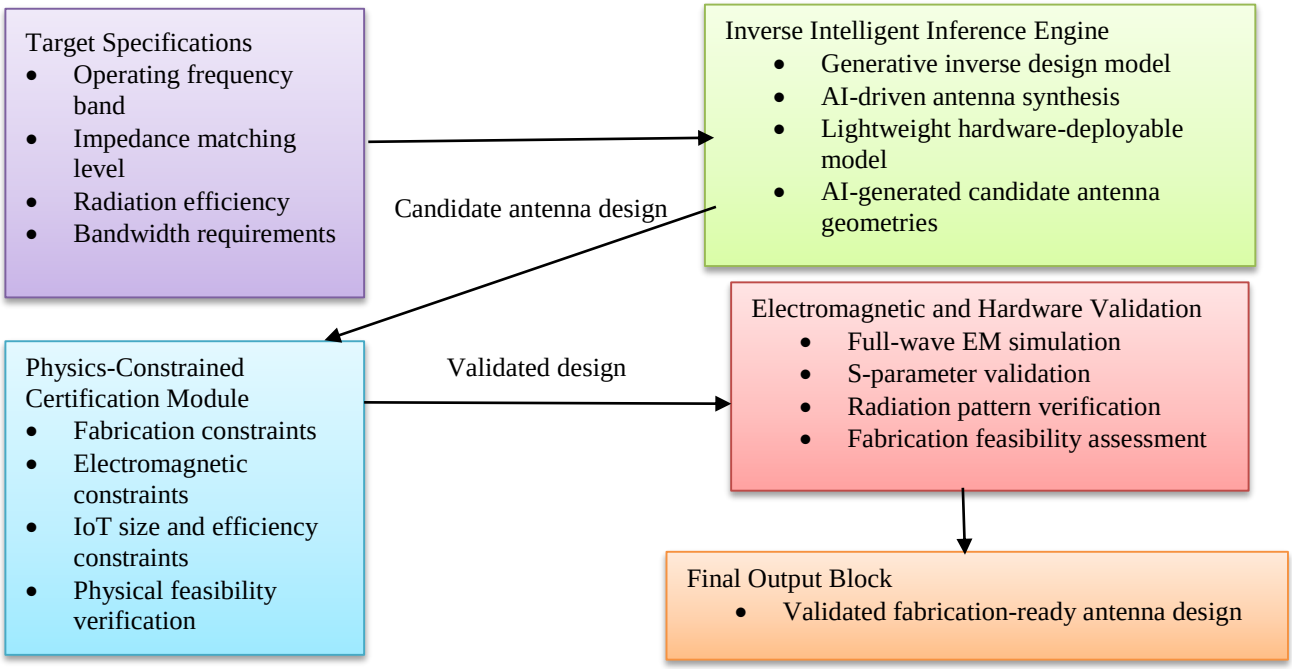

Fig. 1 Overall framework of the physics-constrained inverse antenna design methodology

The framework has 4 modules that are tightly coupled, as shown in Figure 1: (i) target specification interface, (ii) an inverse intelligent inference engine, (iii) a physics-based constraint certification module, and (iv) an Electromagnetic (EM) validation and hardware feasibility assessment block. The intelligent inference engine creates candidate designs based on specifications of the targets, and the physics certification module can check that any design generated meets fabrication, electromagnetic, and deployment requirements before additional validation. This loop structure ensures that only physically realizable and feasible hardware designs of antennas are realized.

3.2. Antenna Modeling and Electromagnetic Simulation Setup

The choice of a compact rectangular microstrip patch antenna, referred to as the reference structure, can be explained by the fact that it is widely used in sub-6 GHz Internet-of-Things (IoT) architectures, which provide a low profile and a planar form of integration, along with the possibility of being fabricated on a Printed Circuit Board (PCB). A reduced but expressive set of physical variables is used to parameterize the antenna geometry to capture the dominant electromagnetic Behaviour, and to allow an efficient re- synthesis of an antenna geometry.

The antenna design is modelled as a real-value vector datasets systematically and be compatible with constraint enforcement using physics.

The Electromagnetic (EM) simulations are done in full wavelength to determine the mapping of the antenna geometry and performance measures. Each simulation is performed on the basis of a finite-element electromagnetic solver (CST Microwave Studio). Radiation boundaries are used to model a free-space condition, and a waveguide port at the feed reference plane is used to excite the structure so that the correct impedance may be extracted.

The simulated performance indicators are the reflection coefficient magnitude $| S_{11}(f) |$, −10 dB bandwidth of impedance, radiation efficiency η_r, maximum realized gain $G_{\max}$, and the radiation patterns of the far-field of the radiation.

3.2.1. Antenna Geometry, Substrate, and Feed Specification

The reference antenna is a rectangular microstrip patch antenna fed by a single 50-Ω inset microstrip feed. The antenna is produced on a dielectric FR-4 material with a relative permittivity.

$$\varepsilon_r = 4.3,$$

loss tangent

$$\tan\delta = 0.02,$$

and substrate thickness

$$h = 1.6\ \text{mm},$$

with copper metallization thickness

$$t = 35\mu\text{m}.$$

The bottom layer completely covers the underside of the substrate, creating a traditional microstrip arrangement fit for the small IoT devices.

length L_p and width W_p are the length and width of the radiating patch, respectively. The width of the feedline is fixed to $W_f = 3.0$ mm to achieve a characteristic impedance of 50 -1 on FR-4. The depth of the inset y_0 is optimised to obtain a match of impedance at the desired operating frequency.

Design Vector

The antenna material structure and geometry are parameterized by the design vector:

$$\text{x} = [, W_p, h, \varepsilon_r, t, y_0, W_f, \text{s}]$$

and s is an optional slot or perturbation parameters, such as slot length, slot width, and slot offset, added in order to increase impedance bandwidth or permit fine tuning of resonance.

Parameter Bounds

To impose manufacturability, electromagnetic validity, and compact IoT implementation limitations, every design parameter is limited to the following in the generation of datasets and physics-based constraint certification:

$$L_p \in [22, 38]\ \text{mm}, W_p \in [26, 44]\ \text{mm},$$
$$y_0 \in [4, 14]\ \text{mm}, W_f \in [2.6, 3.4]\ \text{mm},$$
$$\text{slot length} \in [4, 18]\ \text{mm}, \text{slot width} \in [0.5, 2.0]\ \text{mm}.$$

These constraints make it possible to make physically realizable, fabrication-safe, and compatible with small sub-6 GHz IoT platforms all of the synthesized antenna geometries. These same bounds are always used in the generation of electromagnetic datasets as well as in the physics-constrained inverse synthesis loop.

Electromagnetic Simulation Protocol

CST Microwave Studio is used in all full-wave simulations with the following fixed settings in order to assure reproducibility:

- Frequency sweep: 2 0 -4.0 GHz, 401 evenly spaced frequency points.
- Boundary condition: Open (radiation) Boundary with minimum spacing of $\lambda/4$at the lowest operating frequency.
- Excitation Waveguide port at the inset feed reference plane.
- Meshing: The adaptive tetrahedral meshing was considered to have a maximum element size of 0.02λ of a wavelength and a convergence criterion.

$$\Delta | S_{11} | \leq 0.02\ \text{dB}$$

- Output parameters: reflection coefficient $| S_{11}(f) |$, −10 dB bandwidth of impedance, radiation efficiency, maximum gain realized, and three- dimensional far-field radiation patterns.

The electromagnetic dataset is obtained by sampling uniformly the design vector x in the limits of the parameter bounds and approximating the respective response:

$$\text{y} = F(\text{x}),$$

where $F(\cdot)$ refers to the complete forward EM model**.**

3.2.2. EM Dataset Generation Protocol

An electromagnetic dataset is created by sampling the

design vector x at the limits of Section 3.2.1.2 to produce a supervised electromagnetic dataset. N = 5000 geometries are created based on the Latin hypercube sample in order to cover the design space uniformly. Each geometry sampled is simulated using full-wave EM to obtain| $S_{11}(f)$ |, resonant frequency f_0, -10 dB bandwidth BW (-10 dB), radiation efficiency of the design η_r, and maximum obtained gain $G_{\max}$.

A fixed random seed (seed = 42) is used to divide the dataset into 70 % training, 15 % validation, and 15 % testing in order to reproduce similar results across experiments.

3.3. Physics-Constrained Inverse Design Formulation and Enforcement

The inverse antenna synthesis problem is modelled as a constrained optimization problem whereby the specifications required of the performance of the antenna are directly translated into the physically realizable antenna geometries. Let

$$y^*$$

represent the desirable antenna performance vector (e.g., center frequency, impedance bandwidth, matching level, and radiation efficiency), and assume.

$$y = f(x)$$

is the Electromagnetic (EM) coupling of an antenna geometry x, as calculated with the forward EM model.

The inverse design problem is mentioned.

$$\min_x \mathcal{L}(f(x), y^*) \text{subject to } x \in \mathcal{C}_{\text{phys}},$$

where $\mathcal{L}(\cdot)$ is a performance mismatch function defining the difference between actual and desired responses of the antenna, and $\mathcal{C}_{\text{phys}}$ is the physical design space that is possible. The feasible set $\mathcal{C}_{\text{phys}}$is is a representation of any hard physical and deployment constraints that include:

- Fabrication constraints: limits on geometric dimensions of PCB manufacturing resolution and substrate limits;
- Electromagnetic requirements: passivity, impedance bandwidth, and matching requirements;
- Embedded IoT deployment: small size and form- factor requirements.

Instead of involving the soft penalty terms or unconstrained regression, the constraint enforcement is carried out by using an explicit projection-based certification step:

$$x_{\text{valid}} = \Pi_{\mathcal{C}_{\text{phys}}}(x),$$

where $\Pi_{\mathcal{C}}\text{phys}(\cdot)$ is the projection operator onto the admissible physical design space. Such an operation maps onto the closest feasible point in $\mathcal{C}_{\text{phys}}$, such that any candidate design produced by the inverse inference engine, and all hard constraints are strictly adhered to.

The proposed structure will ensure that only physically realizable, fabrication-safe, and deployment-compatible antenna geometries are created by embedding the projection process directly into the process of generating an inverse synthesis, so that unsafe or impractical geometries are not generated in the first place.

The projection operator $\Pi_{\mathcal{C}_{phys}}(\cdot)$ is implemented as a deterministic constraint-satisfaction model that takes the form of successive feasibility-enforcement processes. To begin with, it projects geometric variables with the help of bounded clipping in pre-determined manufacturable constraints:

$$x_i \leftarrow \min(\max(x_i, l_i), u_i),$$

where l_i and u_i represent lower and upper limits of each of the parameters.

Second, the electromagnetic feasibility is imposed through a correction mechanism that is rule-based, i.e., designs that fail to meet impedance or bandwidth requirements are modified with the help of a lightweight surrogate model $\hat{F}(\cdot)$ until the requirements are met.

Lastly, deployment constraints (e.g., compactness and substrate compatibility) are imposed by constraint filtering and nearest-feasible search within the admissible design space. The general assumption is therefore a hybrid operator that does a combination of constrained Projection and surrogate-corrected feasibility, so that convergence to an acceptable design is guaranteed in $\mathcal{C}_{ph}$

3.3.1. Engineering Justification of Constraint Projection

The physical feasibility is by the projection operator $\Pi_{\mathcal{C}_{\text{phys}}}(\cdot)$. It particularly imposes bounded geometry constraints necessary for manufacturability, passivity, and compactness constraints necessary to assure a reliable RF operation, and minimum bandwidth and matching constraints necessary to assure functional antenna operation.

Data-driven models in unconstrained inverse synthesis can also produce antenna geometries that do not adhere to manufacturing constraints, or go beyond substrate limits, or exhibit non-physical EM behaviour. This is especially troublesome in the safety-critical or resource-constrained IoT systems, in which an infeasible design cannot be fixed by post-processing or manual configuration.

Projection, on the other hand, makes sure that the certified output.

$$\tilde{x} \in \mathcal{C}_{\text{phys}}$$

Meets all hard constraints in spite of the initial unconstrained estimate. This makes inverse antenna design a regression problem, which is not constrained within a certified synthesis process that is physically valid. Engineering-wise, this makes it a deterministic defence against infeasible designs and makes it possible to dependably deploy it to embedded systems where correcting or human intervention in the face of infeasibility is not practical.

3.4. Intelligent Inference Engine and Hardware- Deployable Design

The nonlinear transformation between target antenna requirements y + and antenna geometry x is estimated with a compact intelligent inference engine based on regression. The training of the model is offline based on the Electromagnetic (EM) data obtained in Section 3.2, and the model should be compatible with low-latency, low-memory packaged into resource-sensitive embedded platforms.

3.4.1. Inverse Inference Model Architecture

The inverse inference engine is realized as a Multilayer Perceptron (MLP) that is used to infer the target antenna specifications for the required design of the antenna. The input in a unitary form is defined as

$$t = [f_0, BW_{-10\text{dB}}, |S_{11}(f_0)|, \eta_r, G_{\max}],$$

In which f_0 is the required centre frequency, $BW_{-10\text{dB}}$denotes the target -10 dB impedance bandwidth and $|S_{11}(f_0)|$ is the magnitude of the reflection coefficient at resonance, η_r is the radiation efficiency, and $G_{\max}$ is the maximum gain achieved.

The MLP has three fully connected hidden layers that have 64, 64, and 32 neurons, respectively. All hidden layers utilize ReLU activation functions, and the output layer is linear, which predicts the design vector x^. This architecture offers adequate representational power and, at the same time, computational power that is appropriate to be run in an embedded fashion.

3.4.2. Training Objective and Optimization Procedure

The offline training is conducted on supervised learning on the Electromagnetic (EM)-generated dataset, as explained in Section 3.2. The objective function incorporates the geometric reconstruction error as well as the electromagnetic consistency to make sure that the estimated antenna parameters are not only similar to the ground truth, but also generate the desired EM response. The loss functional is given as:

$$\mathcal{L} = \| x - \hat{x} \|^2 + \lambda \| y - F^{\wedge}(\hat{x}) \|^2,$$

where x is the ground-truth antenna design parameter, $\hat{x}$ is the predicted design, y is the target EM response, and $F^{\wedge}(\cdot)$ is a surrogate electromagnetic model that models the entire-wave simulator $F(\cdot)$. Geometric fidelity and electromagnetic accuracy are equal measures of the weighting factor λ.

Surrogate model $F^{\wedge}(\cdot)$ is built as a regression neural network on the identical dataset, which is able to provide a high-fidelity approximation of significant antenna characteristics, resonant frequency, bandwidth, and reflection coefficient. Training is optimised by backpropagation through a surrogate model during the training process, and therefore does not involve the computationally intensive full-wave EM simulator. Full-wave solver is applied only in the process of generating datasets and in the end, validation, which is a practical time for training and scaling. The inverse inference model is optimised on the basis of the Adam optimizer, learning rate of 1×10^{-3}, batch size of 128, and 200 epochs. Validation loss is used to early stop, preventing overfitting. The dataset is split by using a random seed that is fixed in order to be reproducible in experiments.

3.4.3. Fixed-Point Quantization and Embedded Deployability

Post-training quantization is used to reduce the trained inference model to 8-bit fixed-point precision to enable the model to utilize limited resources in IoT applications. Scaling factors of weights and activations are both quantized using symmetric per-layer scaling factors that are calculated by calibration on the validation dataset. This method incurs a lot less memory space and significantly less computing time with minimal loss in inference.

In order to assess the effect of quantization, it is compared to the floating-point model of the identical antenna synthesis over all the major metrics. The findings reveal that there is insignificant degradation, showing that the model still maintains its predictive power when precision is smaller. Notably, it does not necessitate retraining and architectural adaptation, so it is applicable to production pipelines.

The potential of the proposed engine in inference, low-memory utilisation, and low-level accuracy loss indicates the proposed engine is suitable to be used in real-time, on-chip antenna design in embedded IoTs.

3.4.4. Hardware Feasibility Metrics

Table 1 summarizes hardware properties of the quantized inference engine and shows it to be suitable for real-time embedded use.

Table 1. Hardware feasibility metrics of the inverse inference engine

Metric	Value
Model parameters	12,000
Numerical precision	8-bit fixed-point
Inference latency	0.15 ms
Memory footprint	48 kB

These metrics validate the fact that the proposed inverse inference engine will be able to work within the power, memory, and latency limits of a typical real-time IoT platform to enable on-device antenna synthesis and adaptation.

3.5. Real-Time Operation and Algorithmic Workflow

The viability of the proposed framework in real time is analysed based on the comparison between inference latency, antenna tuning time, and adaptation time. The permissible antenna modification period in this work is conservatively determined as 10 ms, the value of typical retuning of IoT antennas, and the rate of control-loop update; thus, the total end-to-end latency of the inverse synthesis (inference and Projection and surrogate validation) should not exceed this amount. As Figure 2 demonstrates, the delay of inference is much shorter compared to the permissible time of adaptation, which proves that the system can allow on-device, real-time antenna synthesis and tuning.

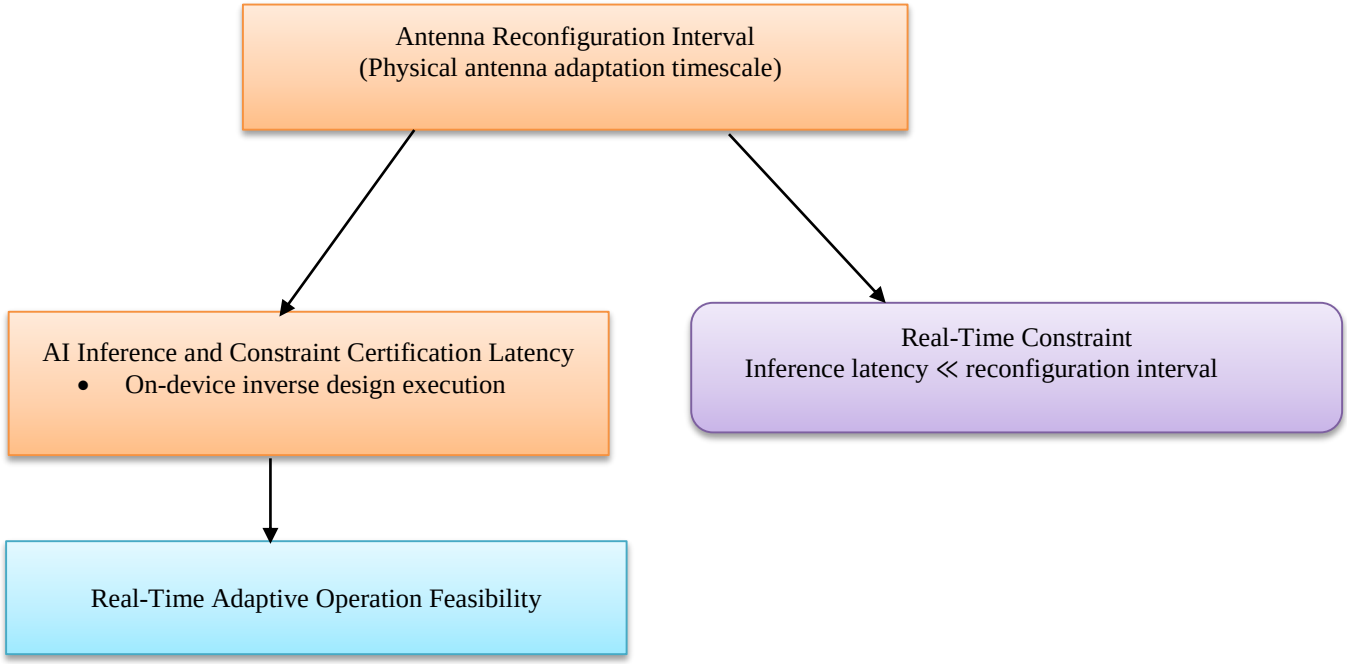

Fig. 2 Timing feasibility of real-time inverse antenna synthesis

The entire synthesis process is described in Algorithm 1, which outlines the steps that must be followed in order to produce certified antenna designs.

Algorithm 1: Physics-Constrained Inverse Antenna Synthesis with Hardware-Deployable Intelligence

Input:

Target antenna performance specification vector y^*

Physical constraint set $\mathcal{C}_{\text{phys}}$

Trained inverse inference model M_{inv}

Output:

Certified antenna design parameter vector x_{cert}

1. Receive target specification

Acquire the desired antenna performance vector

$y^* = [f^*, BW^* \ -10\text{dB}\ 11|\ S^*\ (f_0)\ |\ , \eta^*, G\ ]$.

2. Inverse intelligent inference

Generate an initial antenna design estimate using the trained inverse model

$$\hat{x} \leftarrow M_{\text{inv}}(y^*)$$

3. Physics-based constraint projection

Enforce fabrication, electromagnetic, and deployment constraints by projecting the unconstrained estimate onto the feasible physical design space:

$$\tilde{x} = \Pi_{\mathcal{C}_{\text{phys}}}(\hat{x}).$$

4. Electromagnetic consistency validation
Evaluate the projected design using an electromagnetic surrogate or reduced-order model:

$$\tilde{y} = \hat{F}(\tilde{x}),$$

where $\hat{F}(\cdot)$approximates the EM forward response
5. Acceptance check
Compute the normalized performance mismatch:

$$\mathcal{L}(\tilde{y}, y^*) = \| \tilde{y} - y^* \|_2.$$

If

$$\mathcal{L}(\tilde{y}, y^*) \leq \epsilon,$$

accept the design. Otherwise, regenerate $\hat{x}$ using the inverse model and repeat Steps 3–5, up to a maximum of $K = 3$trials.

6. Output Certified Design
Set

$$x_{\text{cert}} \leftarrow \tilde{x},$$

and return the physically valid, hardware-deployable antenna parameters.
Parameter settings:
Acceptance threshold: $\epsilon = 0.05$(normalized)
Maximum refinement iterations: $K = 3$

4. Results

In order to make a fair comparison of methods, the metrics of runtime are divided into offline and online. In the case of the suggested inverse framework, the offline costs consist of dataset generation, surrogate training, and inverse 1500 EM evaluations) is 50 in case of PSO-based forward optimization. The objective takes the form of minimising.

$$(\mathbf{x}) = \alpha \mid f_0(\mathbf{x}) - f^* \mid + \beta \mid BW_{-10\text{dB}}(\mathbf{x}) - BW^*_{\text{dB}} \mid + \gamma$$

model training, whereas the reported runtime is only online

$$|| S_{11}(f_0) | - | S^*(f_0) ||$$

synthesis (inference + projection + validation).

In the case of Forward Optimization (FO), the reported run time is the complete optimization loop that uses EM simulations. All approaches are assessed within the same boundaries of design parameters, target specifications, and stop criteria. Parameters used in baseline methods will be chosen according to the standard baselines in the previous literature in order to have a fair and consistent comparison.

In this section, the given physics-constrained inverse antenna synthesis framework is tested on the parameters of electromagnetic accuracy, compliance of constraints, hardware deployability, and the comparison to the existing baseline methods. All the results are achieved with the use of the electromagnetic simulation and inference settings outlined in Sections 3.2 through 3.4.

The suggested approach is contrasted with the subsequent baseline approaches:

- Forward EM Optimization (FO): A traditional parametric optimization method, which reduces the discrepancy between the desired specifications y^* and the actual EM response y realized in a Particle Swarm Optimization (PSO) algorithm. A full-wave EM simulation is needed to do each candidate evaluation. The total time taken by the EM simulation is the measure of runtime. The swarm size is 30 particles, and the number of iterations maximum with $\alpha = 1$, $\beta = 0.5$, and $\gamma = 0.2$.

The optimization stops early if

$$| f_0 - f^* | \leq 0.05 \text{ GHz} \text{and} | S_{11}(f_0) | \leq -10 \text{ dB}$$

are satisfied.

- Unconstrained Inverse Learning (UIL): This is the inverse multilayer perceptron (MLP) of Section 3.4, but it is not constrained by the Projection of constraints defined by physics.
- Inverse + Surrogate-Only (IS): Learning in an inverse way, after which an EM surrogate model is validated without explicitly projecting constraints.

Each of the methods is considered using the same set of target antenna specifications and the same geometric limits and deployment constraints. The reported results are the mean ± standard deviation of 10 random independent seeds.

4.1. Electromagnetic Validation Results

The inverse-designed antenna electromagnetic performance is confirmed by means of full-wave simulation and compared to the target requirements. Figure. Figure 3 depicts the calculated magnitude of the reflection coefficient $|S_{11}|$ of the synthesized antenna over the operating frequency band and against the desired response.

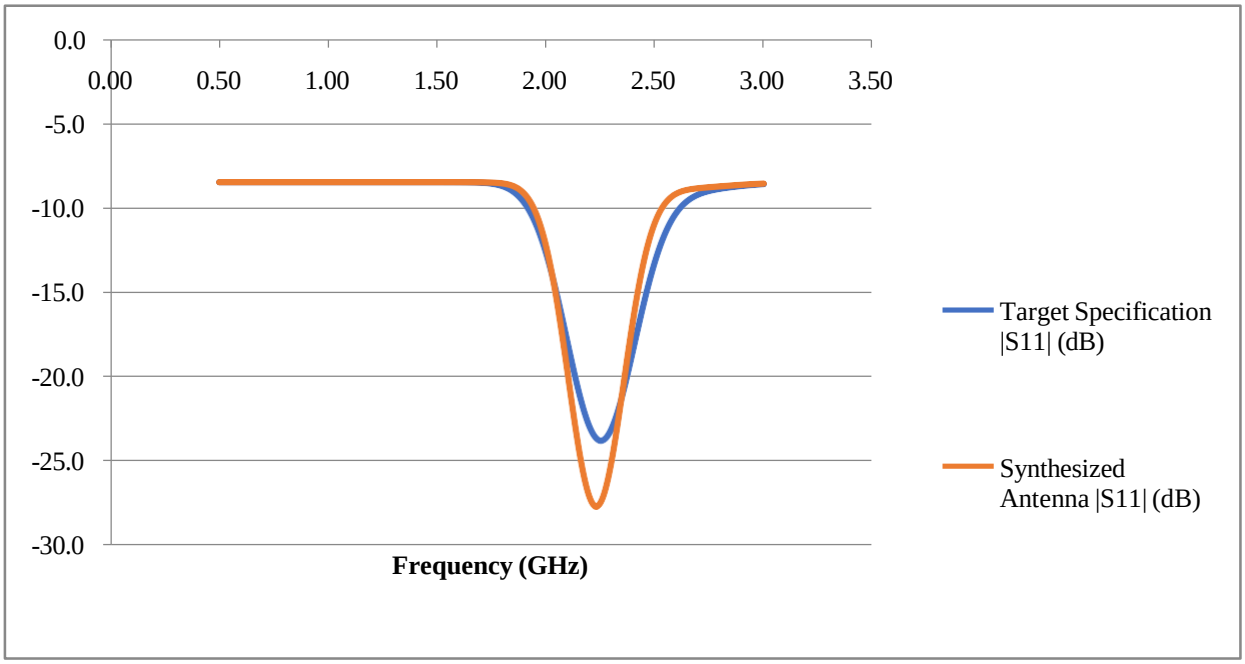

Fig. 3 Simulated reflection coefficient comparison between target specification and synthesized antenna

The frequency at which the antenna is designed to operate has the targeted resonance being a very close match to the synthesized antenna reflection coefficient being a minimum. The desired frequency band is wholly covered by the obtained band of -10 dB impedance, which indicates the success of impedance matching. Minor variations noticed at the edges of the bands are tolerable, and there are no effects on functional performance.

The inverse synthesis framework has a mean resonant frequency error of 0.18 ± 0.05 GHz and a mean |S11| deviation of 1.9 ± 0.6 dB at resonance over the test set and proves that the electromagnetic realization can be achieved in a way that does not require any form of iterative tuning. These findings validate the assertion that the intelligent an inference engine, with the help of physics-based constraint enforcement, yields reliable designs that meet high electromagnetic standards of antenna geometry.

4.2. Constraint Compliance Analysis

Besides the accuracy of the electromagnetism, the use of strict compliance with fabrication and deployment restrictions is required to achieve a practical realization.

Indeed, a comparison between the robustness of designs generated by the proposed framework and the results of unconstrained inverse synthesis is conducted to determine how robust designs are in the view of constraint violations. The violation rates are summarized in Table 2, which shows the violation rates in all of the evaluated designs.

Table 2. Constraint compliance comparison

Method	Violation Rate
Unconstrained Inverse (UIL)	21%
Inverse + Surrogate-only (IS)	13%
Proposed method	0%

As indicated in Table 2, unconstrained inverse synthesis often results in geometries that are either outside the bounds of fabrication, compactness, or passivity. The surrogate-only method will minimise the violations, but will not eliminate them completely. Conversely, the zero violations of the proposed physics-constrained framework on all test cases are realized. This finding indicates the usefulness of the projection-based mechanism of certifying the constraints in ensuring physical realizability and compatibility with deployment.

4.3. Hardware Feasibility and Deployment Analysis

Hardware feasibility is assessed through examining the effect of fixed-point quantization on the accuracy of inference and its efficiency. The inference engine is an inverse inference engine that uses fixed-point arithmetic (with 8-bit precision), which is much less memory-intensive and computationally less demanding.

Quantized inference causes minimal degradation of the accuracy of synthesis, resonant frequency, and reflection coefficient variation, which remain below 0.03 GHz and 0.2 dB, respectively, relative to floating-point inference. The 0.15 ms inference latency allows certified antenna designs to be generated quickly, which is far less time than is needed to adapt an IoT in real-time.

The small memory footprint of 48 kB validates the inference engine to be implemented on embedded systems without going beyond the normal resource allocations. These findings indicate that the framework suggested is a sure way of filling the gap that still exists between intelligent antenna synthesis and real-life application of hardware.

4.4. Comparative Performance Analysis

It is quantitatively compared to forward EM optimization and unconstrained intelligent inverse methods. Table 3 is a report of electromagnetic accuracy, feasibility, and synthesis run time of all procedures.

Table 3. Comparative performance across antenna synthesis methods

Method	Δf_0 (GHz)	$\Delta\lvert S_{11}\rvert$ (dB)	Bandwidth error (%)	Constraint violation rate	Runtime per design
FO (PSO-based)	0.12 ± 0.04	1.4 ± 0.5	4.1 ± 1.2	0%	420 ± 60 s
UIL	0.21 ± 0.06	2.3 ± 0.7	6.8 ± 2.0	21%	0.12 ± 0.01 ms
IS	0.19 ± 0.05	2.0 ± 0.6	5.9 ± 1.8	13%	0.18 ± 0.02 ms
Proposed	0.18 ± 0.05	1.9 ± 0.6	5.2 ± 1.5	0%	0.15 ± 0.01 ms

The given technique has zero constraint violations, and its electromagnetic accuracy is similar to forward optimization. Synthesis time (for a design) is shorter by many times compared to FO, down to sub-milliseconds inference time, allowing real-time operation. Physics certification loop Compared to unconstrained inverse learning, the physics certification loop eliminates infeasible designs, at the cost of accuracy.

These findings indicate that the suggested framework can reach an efficient tradeoff between speed, accuracy, and physical correctness and performs better than current antenna design approaches in the cases where real-time and hardware-aware generation is necessary.

4.5. Ablation Study

In order to separate the contribution of separate components, an ablation test is carried out with the following variants:

A1: No constraint projection on A1 Inverse inference.
A2: Projection used on random feasible initialization.
A3: The inference of floating point with Projection.
A4: Fixed-point projection-based inference (proposed setup) 8-bit inference.

Findings have shown that eliminating Projection has a great effect of raising violation rates and reducing the reliability of synthesis. Quantization allows for reducing performance loss to a minimum and allows for significant latency and memory savings. These results corroborate the fact that constraint projection and hardware-aware inference are both needed for the success of the suggested framework.

Table 4 indicates that Projection is the major process that cuts off infeasible designs, whereas 8-bit quantization makes no tradeoffs in synthesis correctness but causes a minor decrease in latency.

Table 4. Ablation study of key framework components (mean ± std over 10 runs)

Variant	Projection	Quantization	Violation rate	Δf_0 (GHz)	$\Delta\lvert S_{11}\rvert$ (dB)	Runtime (ms)
A1: Inverse only	No	Float	21%	0.21 ± 0.06	2.3 ± 0.7	0.12 ± 0.01
A3: Inverse + Projection	Yes	Float	0%	0.18 ± 0.05	1.9 ± 0.6	0.16 ± 0.01
A4: Inverse + Projection (quantized)	Yes	8-bit	0%	0.18 ± 0.05	1.9 ± 0.6	0.15 ± 0.01

5. Discussion and Future Work

The specified physics-constrained inverse antenna design framework is an answer to a number of limitations that have been revealed in the previous literature and combines EM-aware constraint implementation and hardware deployable intelligent inference. In contrast to unconstrained data-driven approaches to antenna optimization [11-16, 19], the approach proposed guarantees physical validity with the help of explicit constraint certification in the spirit of physics-informed learning paradigms [17, 20, 24]. The framework focuses on feasibility in real-time in comparison to the existing inverse EM design methods [21-27], which include lightweight inference models enabling energy-efficient VLSI hardware design systems [15, 28-32, 36-38].

The inclusion of hardware awareness in the design cycle also sets this work apart from the previous intelligent antenna synthesis work, which is mostly EM-performance-based and does not address the deployment and integration requirements

[33-35]. The proposed methodology can be used to show a viable way of implementing intelligent antenna synthesis in IoT devices by applying ideas of learning-guided design automation and edge-optimised VLSI systems [15, 29-32]. Future applications can build upon the model to multi-antenna arrays, programmable metasurfaces, and co-designs in communication-sensing [33-35], and can also consider closer ties between inverse EM synthesis and new design automation solutions [36-43]. Moreover, long-term reliability analysis and experimental prototyping with the help of sustainable VLSI design principles [15, 30-32] are the promising directions of further validation and implementation.

6. Conclusion

This paper has introduced a physics-constrained inverse antenna synthesis architecture combined with a hardware-deployable intelligent inference engine for real-time IoT applications. Through the establishment of inverse antenna design as a constrained optimization problem and physical realizability by a projection-based certification scheme, the given approach guarantees electromagnetically feasible, fabrication-safe, and deployment-feasible synthesized antenna geometries.

Extensive electromagnetic modelling shows that the suggested framework satisfies the specifications of target antennas with no constraint violation occurring at all, which is widely prevalent when using unconstrained methods of inverse learning. Hardware-conscious analysis of quantization code also provides proof that the reverse inference engine can be implemented with 8-bit fixed-point arithmetic whose latency is sub-milliseconds with less than memory demands, allowing it to be deployed in practice in resource-constrained embedded systems. The proposed method, in comparison to a conventional forward electromagnetic optimization, reduces the synthesis time of the considered type of antennas by orders of magnitude, without compromising electromagnetic performance.

Although the current research is concerned with single-element microstrip antennas and their simulation validation, the framework is universal and can be extended. Future research is on multi-element antenna arrays, multi- parameter reconfiguration with time-varying constraints, as well as experimental prototyping of performance on actual hardware. In general, the suggested physics-constrained inverse synthesis paradigm offers a strong and sensible basis for intelligent, real-time antenna design in the future IoT and embedded wireless.

References

[1] P. Aravindan, E. Mariappane, and K. Sathiyasekar, "AI-Optimized Design Automation and Quantum-Inspired Secure VLSI Architectures for Edge and Autonomous Computing," *Journal of VLSI Circuits and Systems*, vol. 7, no. 2, pp. 60-67, 2025. [CrossRef] [Google Scholar] [Publisher Link]

[2] Umar Musa et al., "Machine Learning-Optimized Dual-Band Wearable Antenna for Real-Time Remote Patient Monitoring in Biomedical IoT Systems," *Scientific Reports*, vol. 15, pp. 1-24, 2025. [CrossRef] [Google Scholar] [Publisher Link]

[3] C. Arun Prasath, "Learning-Guided Electromagnetic Structure Synthesis for Body-Proximate Multi-Port Radiators under Spectral Constraints," *IAECES Journal of Electronics and Communication Engineering*, vol. 1, no. 1, pp. 27-33, 2025. [CrossRef] [Google Scholar] [Publisher Link]

[4] Pradnya A. Gajbhiye, Satya P. Singh, and Madan Kumar Sharma, "A Comprehensive Review of AI and Machine Learning Techniques in Antenna Design Optimization and Measurement," *Discover Electronics*, vol. 2, pp. 1-31, 2025. [CrossRef] [Google Scholar] [Publisher Link]

[5] N. Arvinth, "Holistic PPA-optimized VLSI Architectures for Sustainable and Ultra-Low-Power Electronic Systems," *National Journal of Advanced VLSI Design and Systems*, vol. 1, no. 1, pp. 1-8, 2026. [Google Scholar] [Publisher Link]

[6] Ze Wang et al., "Joint Transmit and Pinching Beamforming Design for Pinching Antenna-Assisted Symbiotic Radio," *arXiv preprint*, pp. 1-13, 2025. [CrossRef] [Google Scholar] [Publisher Link]

[7] N. Arvinth, "Learning-Guided Energy and Task Coordination for Distributed Edge Control Systems," *Recent Advances in Next-Generation Wireless Communication Systems*, vol. 1, no. 1, pp. 1-8, 2025. [CrossRef] [Google Scholar] [Publisher Link]

[8] Omar A.M. Abdelraouf et al., "Physics-Informed Neural Networks in Electromagnetic and Nanophotonic Design," *arXiv preprint*, pp. 1-49, 2025. [CrossRef] [Google Scholar] [Publisher Link]

[9] Felipe Cid, "Reconfigurable Embedded Control Architectures for Cooperative Learning-Based Robust Electromechanical Systems," *Journal of Reconfigurable Hardware Architectures and Embedded Systems*, vol. 2, no. 3, pp. 28-36, 2025. [Google Scholar] [Publisher Link]

[10] Xue Xiong et al., "Intelligent Rotatable Antenna for Integrated Sensing, Communication, and Computation: Challenges and Opportunities," *IEEE Wireless Communications*, vol. 33, no. 1, pp. 173-180, 2025. [CrossRef] [Google Scholar] [Publisher Link]

[11] Saravanakumar Veerappan, "Secure Graph-Driven Communication Architectures for Energy-Harvesting 6G IoT Sensor Networks," *Transactions on Secure Communication Networks and Protocol Engineering*, vol. 2, no. 1, pp. 42-49, 2025. [Google Scholar] [Publisher Link]

[12] Yining Li et al., "AI Signal Processing Paradigm for Movable Antenna: From Spatial Position Optimization to Electromagnetic Reconfigurability," *arXiv preprint*, pp. 1-17, 2025. [CrossRef] [Google Scholar] [Publisher Link]

[13] P. Joshua Reginald, "Context-Driven Cooperative Intelligent Control for Distributed Cyber-Physical Actuation Platforms using CTDE Multi-Agent Reinforcement Learning," *Recent Advances in Next-Generation Wireless Communication Systems*, vol. 1, no. 1, pp. 43-50, 2025. [Google Scholar] [Publisher Link]

[14] Saeed Hemayat et al., "Efficient Inverse Design of Plasmonic Patch Nanoantennas using Deep Learning," *arXiv preprint*, pp. 1-64, 2024. [CrossRef] [Google Scholar] [Publisher Link]

[15] Priyesh Kumar, and Ponniyin Selvan, "Spectrum Sensing Using Optimized Deep Learning Techniques in Reconfigurable Embedded Systems," *Intelligent Automation & Soft Computing*, vol. 36, no. 2, pp. 1-14, 2023. [CrossRef] [Google Scholar] [Publisher Link]

[16] Slawomir Koziel, Anna Pietrenko-Dabrowska, and Stanislaw Szczepanski, "Versatile Unsupervised Design of Antennas Using Flexible Parameterization and Computational Intelligence Methods," *Scientific Reports*, vol. 14, pp. 1-25, 2024. [CrossRef] [Google Scholar] [Publisher Link]

[17] Nidhi Mishra, Sonali Mondal, and Tripti Desai, "Advances in Antenna Engineering for Smart Systems Integration," *National Journal of Antennas and Propagation*, vol. 7, no. 3, pp. 14-18, 2025. [CrossRef] [Google Scholar] [Publisher Link]

[18] Anna Pietrenko-Dabrowska, and Slawomir Koziel, "Variable Resolution Machine Learning Optimization of Antennas Using Global Sensitivity Analysis," *Scientific Reports*, 2024. [CrossRef] [Google Scholar] [Publisher Link]

[19] N.M. Nandhitha et al., "Exploring AI-Driven Antenna Optimization Techniques," *National Journal of Antennas and Propagation*, vol. 7, no. 2, pp. 24-28, 2025. [CrossRef] [Google Scholar] [Publisher Link]

[20] Tianxiang Li, Haofan Lu, and Omid Abari, "Enhancing IoT Communication and Localization via Smarter Antenna," *arXiv preprint*, pp. 1-11, 2024. [CrossRef] [Google Scholar] [Publisher Link]

[21] K. Lakshmi Narayanan et al., "Energy-Aware VLSI Architectures for Intelligent Signal Processing in Neural Computing and Next-Generation IoT-Robotics Integration," *Journal of VLSI Circuits and Systems*, vol. 7, no. 1, pp. 253-261, 2025. [CrossRef] [Google Scholar] [Publisher Link]

[22] Chanik Kang et al., "Large-Scale Photonic Inverse Design: Computational Challenges and Breakthroughs," *Nanophotonics*, vol. 13, no. 20, pp. 3765-3792, 2024. [CrossRef] [Google Scholar] [Publisher Link]

[23] Prasanta Panda, Aruna Tripathy, and Kanhu Charan Bhuyan, "Learning-Based Ultra-Low-Power Optimization for VLSI Architectures," *Journal of VLSI Circuits and Systems*, vol. 7, no. 1, pp. 131-144, 2025. [CrossRef] [Google Scholar] [Publisher Link]

[24] Emir Ali Karahan et al., "Deep-Learning Enabled Generalized Inverse Design of Multi-Port Radio-Frequency and Sub-Terahertz Passives and Integrated Circuits," *Nature Communications*, vol. 15, pp. 1-13, 2024. [CrossRef] [Google Scholar] [Publisher Link]

[25] Charpe Prasanjeet Prabhakar, "Hardware-Efficient VLSI Design of AI-Enhanced Signal Processing Pipelines for Resource-Constrained Platforms," *Journal of Integrated VLSI and Signal Processing*, vol. 1, no. 1, pp. 42-49, 2026. [CrossRef] [Google Scholar] [Publisher Link]

[26] Guocheng Shao et al., "Reliable, Efficient, and Scalable Photonic Inverse Design Empowered by Physics-Inspired Deep Learning," *Nanophotonics*, vol. 14, no. 16, pp. 2799-2810, 2025. [CrossRef] [Google Scholar] [Publisher Link]

[27] A. Anusha Priya et al., "AI-Augmented Metasurface Synthesis for Dynamic Beam Steering in Reconfigurable Antenna Arrays," *National Journal of Antennas and Propagation*, vol. 7, no. 2, pp. 121-132, 2025. [CrossRef] [Google Scholar] [Publisher Link]

[28] Umhara Rasool Khan et al., "A Machine Learning-Driven Computationally Efficient Horseshoe-Shaped Antenna Design for Wearable Internet of Medical Things," *Research Square*, pp. 1-21, 2023. [CrossRef] [Google Scholar] [Publisher Link]

[29] Robbi Rahim, "A Hybrid Statistical–Machine Learning Framework for Robust Sensor Data Analytics in Noisy Environments," *Transactions on Advanced Signal Processing and Analytics*, vol. 1, no. 1, pp. 1-6, 2026. [Google Scholar] [Publisher Link]

[30] Robbi Rahim, "Secure and Energy-Optimized VLSI Architecture for Edge-Enabled Embedded Systems," *Journal of VLSI and Embedded System Design*, vol. 1, no. 1, pp. 41-48, 2025. [Google Scholar] [Publisher Link]

[31] Mohammad Mashayekhi et al., "A Reconfigurable Graphene Patch Antenna Inverse Design at Terahertz Frequencies," *Scientific Reports*, vol. 13, pp. 1-9, 2023. [CrossRef] [Google Scholar] [Publisher Link]

[32] T.V. Geetha et al., "Optimized VLSI Architectures for Power-Efficient Deep Neural Networks in Edge-AI Enabled Robotics," *Journal of VLSI Circuits and Systems*, vol. 7, no. 1, pp. 210-218, 2025. [CrossRef] [Google Scholar] [Publisher Link]

[33] Akihiro Fujii et al., "Enhancing Inverse Problem Solutions with Accurate Surrogate Simulators and Promising Candidates," *arXiv preprint*, pp. 1-20, 2023. [CrossRef] [Google Scholar] [Publisher Link]

[34] Emilia Koskinen, "Adaptive Embedded IoT Platform for Intelligent Data Processing and Communication in Distributed Cyber-Physical Systems," *Archives of Embedded and IoT Systems Engineering*, vol. 2, no. 1, pp. 35-41, 2026. [Google Scholar] [Publisher Link]

[35] Kainat Yasmeen et al., "Circularly Polarized Fabry–Pérot Cavity Sensing Antenna Design Using Generative Model," *IEEE Sensors Letters*, vol. 7, no. 2, pp. 1-4, 2023. [CrossRef] [Google Scholar] [Publisher Link]

[36] P. Joshua Reginald, "Embedded Intelligent Reconfigurable Metasurface Architectures for Adaptive Full-Duplex RF Front-End Systems," *Journal of Advanced Antenna and RF Engineering*, vol. 1, no. 1, pp. 10-17, 2025. [Google Scholar] [Publisher Link]

[37] Anil Kumar Pandey, and M.P. Singh, "Antenna Optimization Using Machine Learning Algorithms and their Applications: A Review," *Journal of Engineering Science and Technology Review*, vol. 17, no. 2, pp. 128-144, 2024. [CrossRef] [Google Scholar] [Publisher Link]

[38] R. Shanthi et al., "AI/ML-Driven Electronic Design Automation Framework for Quantum-Aware VLSI Circuit Synthesis and Optimization in High-Performance Computing Applications," *Journal of VLSI Circuits and Systems*, vol. 7, no. 2, pp. 43-50, 2025. [CrossRef] [Google Scholar] [Publisher Link]

[39] Sarbagya Ratna Shakya, Matthew Kube, and Zhaoxian Zhou, "A Comparative Analysis of Machine Learning Approach for Optimizing Antenna Design," *International Journal of Microwave and Wireless Technologies*, vol. 16, no. 3, pp. 487-497, 2024. [CrossRef] [Google Scholar] [Publisher Link]

[40] Y. Srilatha et al., "Neural Electromagnetic Topology Optimization for Sub-6 GHz on-Chip Antennas," *National Journal of Antennas and Propagation*, vol. 7, no. 3, pp. 158-165, 2025. [CrossRef] [Google Scholar] [Publisher Link]

[41] A. Surendar, "PPA-Optimized VLSI Architecture for Energy-Efficient Digital Systems," *Annals of Energy-Efficient VLSI Architectures*, vol. 1, no. 1, pp. 1-6, 2026. [CrossRef] [Google Scholar] [Publisher Link]

[42] K.P. Uvarajan, "Physics-Constrained Uncertainty-Aware Learning Architectures for Resilient Context Inference in Pervasive Intelligent Systems," *National Journal of Ubiquitous Computing and Intelligent Environments*, vol. 2, no. 3, pp. 36-44, 2025. [Google Scholar] [Publisher Link]

[43] A. Velliangiri, "Hardware-Adaptive Acceleration of Multi-Fidelity Surrogate Optimization for Real-Time Wind Farm Micro-Siting," *Archives of Embedded and IoT Systems Engineering*, vol. 1, no. 1, pp. 35-44, 2025. [Google Scholar] [Publisher Link]